Available online at www.sciencedirect.com
ScienceDirect
Trans. Nonferrous Met. Soc. China 27(2017) 312−323
Transactions of Nonferrous Metals Society of China
www.tnmsc.cn

Tensile, compressive and wear behaviour of self-lubricating sintered magnesium based composites

P. NARAYANASAMY[1], N. SELVAKUMAR[2]

1. Department of Mechanical Engineering, Kamaraj College of Engineering and Technology, Virudhunagar 626001, Tamilnadu, India;
2. Department of Mechanical Engineering, Mepco Schlenk Engineering College, Sivakasi 626005, Tamilnadu, India

Received 14 February 2016; accepted 6 September 2016

Abstract: The graphite (Gr)/MoS_2 reinforced Mg self-lubricating composites were prepared through powder metallurgy. The composites were characterized for microstructure, physical, mechanical and wear properties. Gr/MoS_2 phase in the composites was identified by XRD analysis. Microstructural observation showed that the Gr/MoS_2 particles were homogeneously dispersed within the magnesium matrix. Micro-hardness was measured using an applied load of 5 g with a dwell time of 15 s at room temperature. Hardness of all the composites was measured to be in the range of VHN 29−34. The mechanical properties were studied using micro-hardness, tensile and compression tests. A fractographic analysis was performed using scanning electron microscope. The highest values of hardness, compressive strength and tensile strength were attained using Mg−10MoS_2 composite. A pin-on-disk tribometer was used to measure the friction coefficient and the wear loss of the sintered composites. In addition to that, the friction and wear mechanism of the composites were systematically studied by worn surface characterization and wear debris studies using SEM analysis. The reduced friction coefficient and wear loss were achieved in MoS_2 rather than Gr.

Key words: magnesium composites; self-lubricating; powder metallurgy; sliding wear; microstructure; mechanical properties

1 Introduction

Magnesium is the sixth most abundant element in the earth's crust (2%) and the third most dissolved minerals in seawater (1.1 kg/m^3) [1]. Magnesium is the lightest of all engineering metals with a density of 1.74 g/cm^3, which is two-thirds the density of aluminium and over four times lighter than steel [2]. This property attracts automobile manufacturers to change from denser materials, not only steel, cast iron, copper and titanium but even aluminium, to magnesium [3]. Magnesium has excellent specific strength and stiffness, exceptional dimensional stability, high damping capacity and high recyclability [4]. Based on these superior properties, the research and development of magnesium alloys for practical industrial applications in automotive, aircraft and electronic consumer products have increased worldwide during the past decade [5,6]. The major advantage of magnesium composites lies in the tailorability of their mechanical and physical properties to meet specific design criteria [7].

Wear is one of the most commonly encountered industrial problems that leads to the replacement of components and assemblies in engineering. When two solid surfaces are placed in solid-state contact, it is not easy to envision the absence of some wear even in the most efficiently lubricated systems because of asperity contact [8].

Graphite (Gr) and molybdenum disulphide (MoS_2) are important solid lubricants, and they have a layered structure [9,10]. The layer consists of flat sheets of atoms or molecules, which is called a layer-lattice structure. An important effect is that the materials can shear more simply parallel to the layers than across them. Therefore, they can support relatively heavy loads at right angle to the layers while still being able to easily slide parallel to the layers. This property is being effectively used in lubrication process. The friction coefficient is more or less equal to the shear stress parallel to the layers divided by the yield stress or hardness perpendicular to the layers [11,12]. Because

Corresponding author: P. NARAYANASAMY; Tel: +91-9894514926; E-mail: narayananx5@gmail.com
DOI: 10.1016/S1003-6326(17)60036-0

low friction only occurs parallel to the layers, it follows that these solid lubricants will only be effective when their layers are parallel to the direction of sliding. It is also significant that the solid lubricant should adhere strongly to the bearing surface; otherwise it would be easily rubbed away and give very short service life.

Solid lubricants are used as a powder or thin film to give protection from smashing during relative movement and to decrease friction and wear. Solid lubrication can be implemented where unusual circumstances exist which make lubrication oils and greases unsuitable. For example, in space applications, lubricating oils are shunned due to their out gassing under vacuum and high temperature conditions [13]. Other application areas include the food and textile industries and in tablet manufacturing, where products are likely to become contaminated with oils and greases. According to the scientific periodicals on tribology, graphite is the most widely used solid lubricant in powder materials, followed by molybdenum disulphide. They are important solid lubricants, and have a layered structure [14,15].

Significant efforts have been made to improve the wear resistance of aluminum alloy matrices by the addition of lubricating particles. Aluminium alloy−graphite particulate composites have importance as a self-lubricating material through the enhancement of the wear resistance, machinability and delayed onset of severe wear and seizure. The reduction in wear resistance happens with the addition of graphite, assistances in the formation of a solid lubricating film. This lowers the friction coefficient and increases the anti-seizure quality of the matrix alloy [15,16].

When using copper matrix under unlubricated conditions, it is important to note that copper is more likely to scuff because it is significantly softer and more ductile than common steel. Scuffing may be avoided by using a solid lubricant, which can separate the sliding metallic surfaces [17,18]. Solid lubricants may be delivered to the friction contact if they are included in the copper as the second structural phase. Thus, the coefficient of friction and wear rate depend on the amount of the solid lubricant particles present in the copper matrix. Copper–graphite sintered materials combine the effective electrical conduction of the copper matrix with the self-lubricating ability of graphite to produce good friction and wear performance. These materials can potentially be used as sliding electrical contacts. Higher quantities of solid lubricants, however, contribute to the reduction of wear resistance. The MoS_2 particles, which serve as a lubricant during dry sliding processes, decrease wear loss [19]. There are far fewer studies of molybdenum disulfide with copper and aluminium matrix powder compositions than those of graphite containing materials.

In manufacturing metal matrix composites, the dispersion of the reinforcement particles is a challenge. However, a uniform mixture of metal and non-metal compositions is impossible to obtain by traditional casting methods. Powder metallurgy overcomes the negative effects of liquid state processing methods such as stir casting [20]. Powder metallurgy processing may be used to obtain metallic composite materials containing solid lubricants. In powder metallurgy, the reinforcement is homogeneously dispersed in the matrix for the fabrication of composites [21].

Only a very few researchers have attempted to study the effects on the tribological properties of magnesium self-lubricating composites [22]. Therefore, magnesium matrix composites reinforced with solid lubricants are promising materials that should have good performance in tribo-mechanics, but lead to a reduction in hardness of the composites. An attempt has been made to estimate the dry sliding friction and wear behaviour of Mg−Gr and Mg−MoS_2 self-lubricating composites over a range of loads. The function of solid lubricants (Gr/MoS_2) in dry sliding conditions at room temperature was discussed. In addition, the self-lubricating composites were tested for uniaxial tensile and compressive strength.

2 Experimental

2.1 Powder preparation

The composites were prepared using the powder metallurgy route. To conduct the present study, different types of self-lubricating composites were prepared (Table 1).

Table 1 Details of composition and density values

Composition/%	Theoretical density/(g·cm^3)	Actual density/(g·cm^3)
Pure Mg	1.73	1.65
Mg−5Gr composite	1.77	1.67
Mg−10Gr composite	1.79	1.68
Mg−5MoS_2 composite	1.91	1.81
Mg−10MoS_2 composite	2.07	1.97

In this experiment, magnesium powders with mean particle size of 55 μm were used as the matrix material, and the graphite and molybdenum disulfide powders had mean particle sizes of 25 μm of 99.8% purity and 15 μm of 99.2% purity, respectively. The SEM images of the received magnesium, graphite, and molybdenum disulphide powder particles are shown in Fig. 1, respectively. The Mg particles had spherical and ellipsoidal shapes. The graphite was in the shape of flakes, and the MoS_2 particles had a layer shape. The powders were mixed in a planetary ball mill using

tungsten carbide balls with a diameter of 10 mm and a ball to powder mass ratio of 10:1.

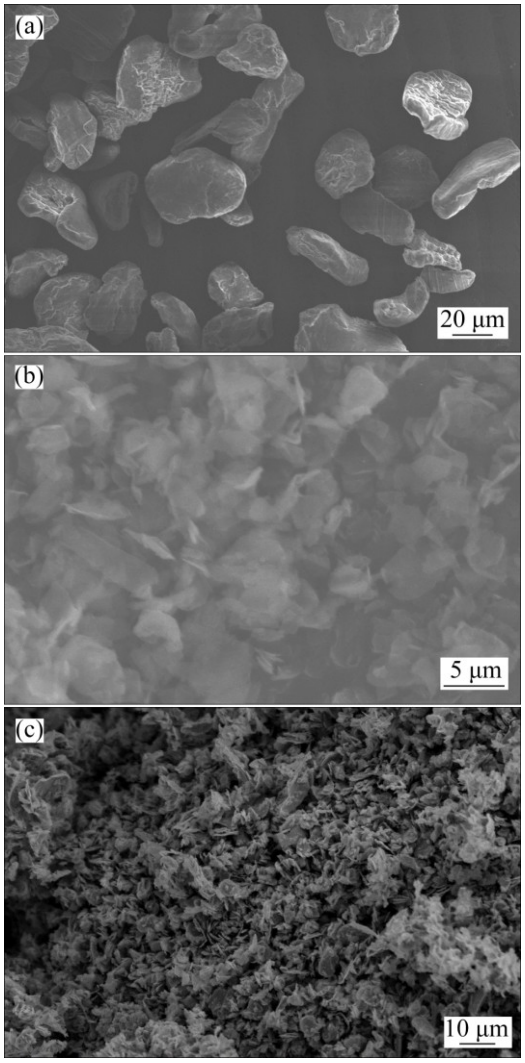

Fig. 1 SEM images of Mg powders (a), Gr particles (b) and MoS_2 particles (c)

The phase evolution of the mixed powders was studied using a high-resolution X-ray diffractometer with a scan speed of 0.01 (°)/s. A Cu K_α radiation source (λ=1.54060 Å) that generates X-ray was used to obtain diffraction patterns for the samples. The mixed powder samples were cleaned with acetone and dried in air prior to the X-ray diffraction studies. The XRD patterns of the ball-milled powders are shown in Fig. 2. The obtained Bragg angles were matched with standard values for Mg, Gr and MoS_2. High intensity Mg peaks can be prominently seen in Fig. 2(a), and the XRD pattern shows the presence of Mg. A clearly visible carbon peak can be observed in the XRD patterns of Mg−Gr composite shown in Fig. 2(b). MoS_2 peaks can be clearly observed in the XRD patterns of Mg−MoS_2 composite shown in Fig. 2(c). The larger peaks in the XRD results signify the presence of Mg, and the smaller peaks show the presence of the solid lubricants (Gr and MoS_2). The absence of oxygen in the composite samples throughout the milling process can be observed in Fig. 2.

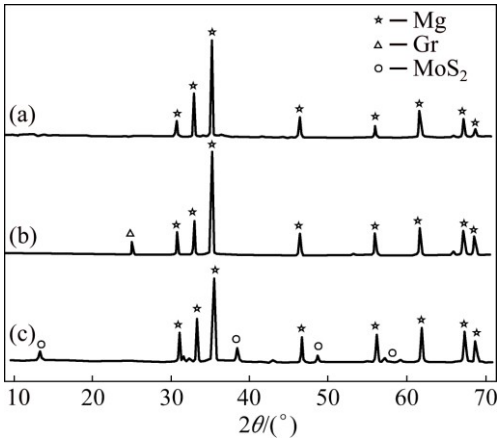

Fig. 2 XRD patterns of mixed composite powders Mg (a), Mg−Gr (b) and Mg−MoS_2 (c)

2.2 Effect of processing parameters on relative density

The effects of compaction pressure and sintering temperature on the properties of the relative density were studied. The literal compaction pressure and sintering temperature reduced the porosity and improved the densification. Diffusion of the atoms is dependent on the compaction pressure and sintering temperature, so that under proper conditions, homogenization and grain growth are activated. Grain growth was directly proportional to the compaction pressure and sintering temperature. The relationships among the relative density and the compaction pressure and sintering temperature are shown in Fig. 3. It should be noted that sintering at a temperature of 530 °C with compaction pressures of 740, 760 and 780 MPa is of consequence at higher relative densities (Fig. 3). As the sintering temperature rises from 500 to 620 °C, the relative density of the composite

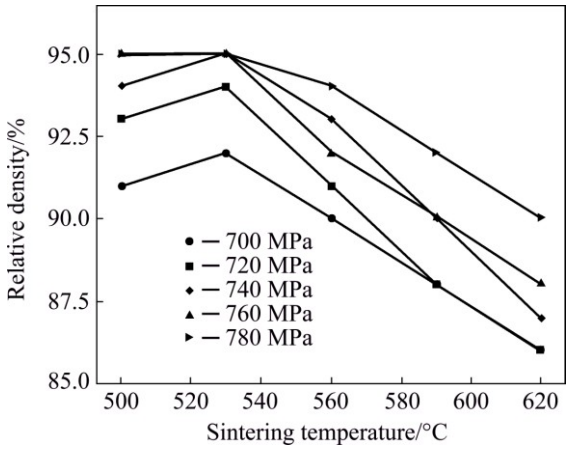

Fig. 3 Effect of compaction pressure and sintering temperature on relative density

increases and then drops to lower values. In comparison, when the sintering temperature beyond 530 °C is employed, the porosity among them is noticed, resulting in a reduced relative density under such circumstances. This phenomenon may be attributed to low specific surface. Since porosity is related to density, by an increase in sintering temperature, the relative density decreases. It can be concluded that the relative density in the sample was higher at 740 MPa and 530 °C. Further increase in the compaction pressure and sintering time has the same or less effect on the relative density.

2.3 Compaction and sintering

After mixing the elemental powders, the mixture was heated in an oven up to 120 °C for 2 h to evaporate the volatile matter in the mixture. The mixed powders were then pressed uniaxially in a hydraulic press at 740 MPa to obtain green compact cylinders with diameter of 17 mm and height of 30 mm. Zinc stearate was used as the die wall lubrication and was manually applied before each run. Before sintering, the outer surfaces of the green compact cylinders were coated with the developed alumina−colloidal graphite mixture and allowed to dry under a room-temperature condition. The green compact cylinders were sintered in a muffle furnace at 530 °C for 1 h and allowed to cool to room temperature in the furnace (Fig. 3). To ensure purification and to eliminate any traces of oxygen contamination, a tray containing carbon was inserted into the furnace [23,24].

2.4 Density values

The Archimedes technique was used to calculate the density of the sintered samples according to ASTM B962−08. The density of the samples was logged using a high precision digital electronic weighing balance with an accuracy of 0.0001 g. All of the samples were tested three times to more precisely determine the density. The density results are consolidated and presented in Table 1. From Table 1, it can be observed that the densities of the composites increased with the addition of reinforcement particles. The Mg−10MoS_2 composites exhibited higher densities than those of the Mg−10Gr composites.

The relative density of the self-lubricated magnesium composites decreased as the Gr and MoS_2 contents increased because the amount of porosity was increased by increasing the pore size, and in addition, there was huge difference in the melting point of the matrix and reinforcements. The relative density of the MoS_2 reinforced magnesium composite was higher than that of graphite reinforced magnesium composite.

2.5 Microstructural characterization

To study the distribution of the Gr and MoS_2 reinforcements in the Mg self-lubricating composites, microstructural characterization studies were performed on top surfaces of the metallographically polished samples using an optical microscopy and the following procedures. The ends of the sintered specimens were conventionally polished with consecutive abrasive papers of grades 600, 800, 1000 and 2500 and finally the polishing was performed using a 1 μm diamond paste suspended in distilled water in a mechanical polishing machine, in order to obtain mirror-like surface finishes.

2.6 Micro-hardness test

The Vickers hardness testing machine is a device that indicates the micro-hardness of a material using a square-shaped base and a pyramidal-shaped diamond indenter with a phase angle of 136°, usually by measuring the effect on the material surface in a localized penetration. The micro-hardness values of the polished samples were measured using applied loads of 5 g with dwell time of 15 s in accordance with ASTM E3 84–99. For each specimen, no fewer than five tests were conducted to obtain repeatable values. The mean value was used.

2.7 Tensile behaviour

To examine the self-lubricating behaviour of the Mg composites, tensile tests were conducted on the Mg−Gr and Mg−MoS_2 composites that had 5% and 10% contents. A hydraulic tensile testing machine (Madurai Engineering works, Tamilnadu) was used to determine the tensile properties of the self-lubricating Mg composites, in accordance with ASTM test method E8M−96. The tensile test was conducted on the sintered samples with a crosshead speed of 1×10^{-3} s^{-1}. The specimens had 10 mm in diameter, 15 mm in gauge length and 25 mm in total length. For each composition, no fewer than three tests were conducted to obtain repeatable values.

2.8 Compressive behaviour

A compressive test was carried out at room temperature on a universal testing machine. Specimens with aspect ratio of 2:1, following ASTM E9−89a, were taken from the sintered samples to assess their compressive properties. The compressive tests were undertaken using a constant cross-head speed and a strain rate of 1×10^{-4} s. The cylindrical specimens were machined to 10 mm in diameter and 20 mm in length. The sintered specimens were subjected to compressive loads until cracks became visible. The initial diameters (D) and initial heights (h) of the specimens were measured and recorded. For each composition, three samples were tested to ensure repeatable values. To provide insights into the various possible fracture

mechanisms operating during the compression loading of the sintered compression test specimens, the fractured surfaces of the compression test specimens were effectively characterized by SEM.

2.9 Tribological behaviour

The friction and wear properties of the composites were tested at room temperature using a pin-on-disc tribometer with applied loads of 2, 5, 10 and 15 N at a constant sliding speed and distance of 3.14 m/s and 2200 m, respectively, and a track radius of 60 mm in an EN31 steel as counterface with a rotational speed of 500 r/min. The dry sliding wear tests were performed using the pin-on-disk equipment with 20 mm long composite pins of 10 mm in diameter in accordance with ASTM G99−05. The tribological performances of the composites were considered as a function of the sliding load. Before and after each test, the specimen and counter disc face were cleaned with acetone to remove trace contaminants. The pin was weighed before and after testing to an accuracy of 0.0001 g to determine the amount of wear loss. Each test was repeated three times, and the average of the results was taken. The frictional force was recorded during the experiment, and friction coefficient was calculated by dividing the frictional force by the applied load. After the wear tests, the worn surfaces of the wear tracks and wear debris were examined by SEM to establish the possible wear mechanisms.

3 Results and discussion

3.1 Microstructure characterization

The outer peripheries of the sintered specimens were soft and free from macro cracks. Typical optical micrographs of the pure Mg, Mg−Gr and Mg−MoS_2 composites are shown in Fig. 4. Figure 4(a) shows the microstructure of a sintered magnesium sample. Figures 4(b)−(c) illustrate that there is no agglomeration of the magnesium with 5Gr and 5MoS_2 particles in the

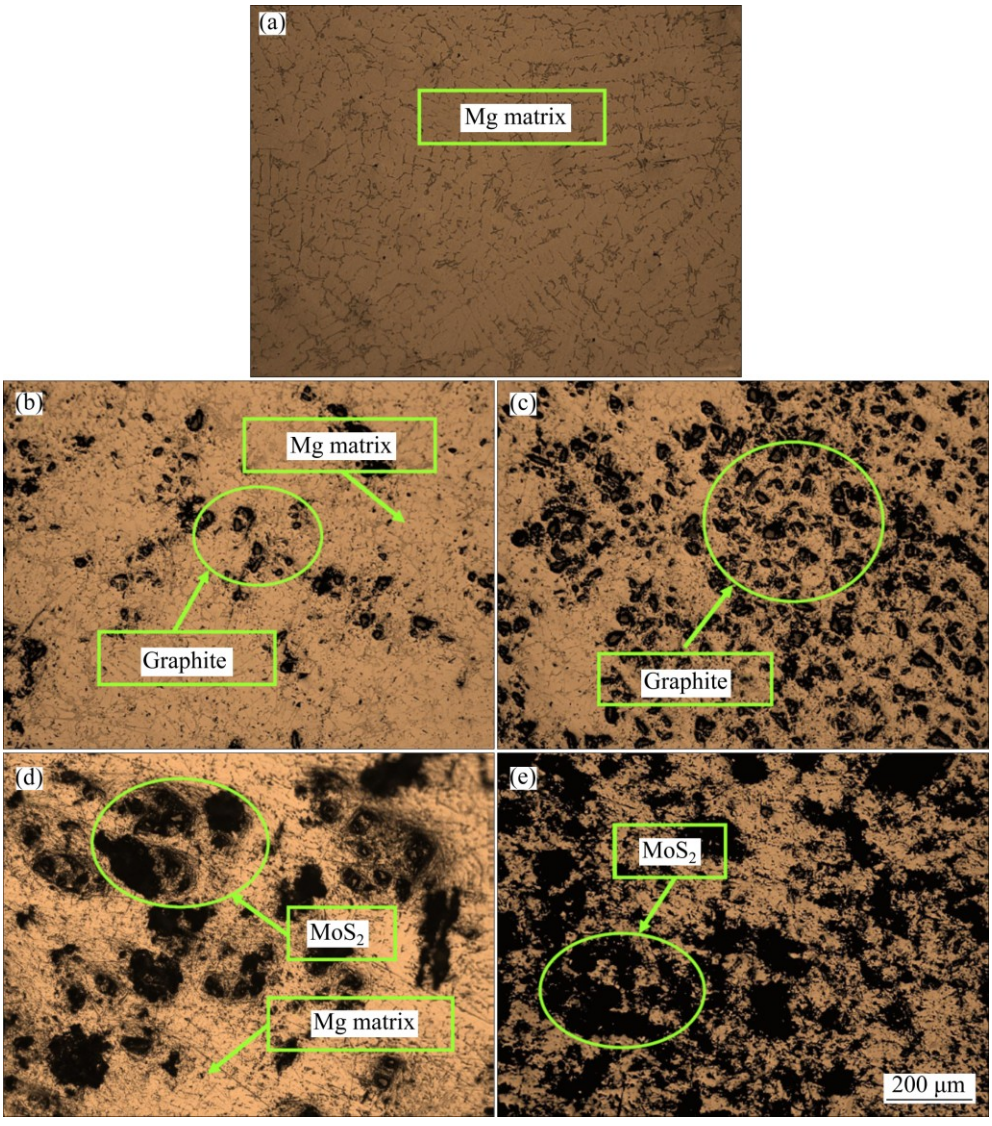

Fig. 4 Optical micrographs of sintered Mg (a), Mg−5Gr (b), Mg−10Gr (c), Mg−5MoS_2 (d) and Mg−10MoS_2 (e)

matrix. It can be observed that there was a homogeneous distribution of Gr particles in the magnesium matrix, and MoS_2 particles in the magnesium matrix with good interfacial bonding between the reinforcing particles and matrix were also observed. In addition, the optical micrographs show that there are no pores and cracks. The Gr and MoS_2 particles were homogeneously distributed along the magnesium matrix when the reinforcement content was 10%, but many agglomerates and clusters can be observed in Figs. 4(d) and (e). The agglomerations of the reinforcement particles may be a consequence of the inadequate ratio of the surface area flanked by the magnesium matrix powders and reinforcement particles.

3.2 Micro-hardness

The results of the hardness tests of the consolidated Mg and Mg−Gr and Mg−MoS_2 self-lubricated composites are presented in Fig. 5. It was found that the micro-hardness increased with an increase in the content of the MoS_2 reinforcement and decreased with the content of Gr. The Mg−MoS_2 composites exhibited higher hardness when compared with the Mg−Gr composites for the same mass fraction, as shown in Fig. 5. The addition of 10MoS_2 increased the hardness, which was contributed to the increased strength compared with the Mg and Mg−Gr composites. The addition of Gr to the magnesium matrix led to a reduction in the hardness of the composites because of its softness.

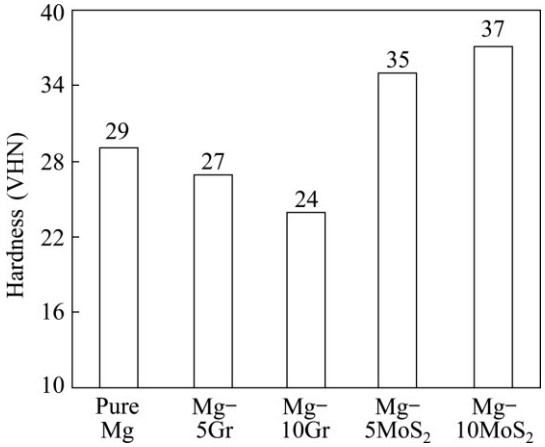

Fig. 5 Micro-hardness of prepared samples

3.3 Tensile fractography

The tensile engineering stress–strain curves of the sintered magnesium and self-lubricating composite samples are shown in Fig. 6, and from the stress–strain curves, in comparison with pure Mg, the addition of MoS_2 to the Mg led to an increase in the tensile yield and ultimate tensile strength. It can be observed from Fig. 6 that the tensile strength of pure magnesium was enhanced with increase in the mass fraction of MoS_2. The addition of Gr slightly decreased the tensile yield strength and ultimate tensile strength when compared with pure Mg. This reduction of tensile properties may be attributed to cracking at the matrix−particulate interface. Figure 6 confirms a reduction in tensile properties with the addition of graphite particulates and Fig. 5 also confirms with no significant change in hardness. Tensile fracture surfaces of all of the test materials after tensile loading are shown in Fig. 7. Fractures occurred in the pure Mg, Mg−5Gr and Mg−10Gr composites (Fig. 7) by mixed mode fracture with a leading cleavage type fracture. However, the Mg−5MoS_2 and Mg−10MoS_2 composites (Fig. 7) demonstrated ductile fracture features. The addition of MoS_2 solid lubricant resulted in the formation of self-lubricating composites and improved the tensile strength as well as the ductility.

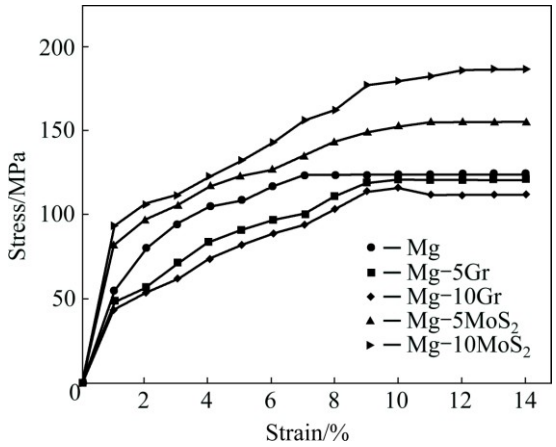

Fig. 6 Engineering stress–strain curves of prepared magnesium samples

3.4 Compressive behaviour

The effects of the addition of self-lubricating particles (Gr and MoS_2) to a magnesium matrix on its compressive strength are shown in Fig. 8. Moreover, the addition of self-lubricating particles to the matrix, increased the compressive strength; this may be due to the addition of Gr/MoS_2 into the Mg matrix. Figure 9 shows the SEM images of fractured surfaces of the Mg, Mg−5Gr, Mg−10Gr, Mg−5MoS_2 and Mg−10MoS_2 composites. Fractures occurred at ~45° with respect to the compression test axis in all of the samples. The fractographic images of the pure Mg and Mg self-lubricating composites showed the presence of shear bands. It has been stated that the compressive failure of pure magnesium is usually brittle because of cleavage fracture (Fig. 9(a)). The fracture surfaces of the Mg−5Gr and Mg−5MoS_2 composites show little cleavage and stream-like patterns that are known as quasi cleavage (Figs. 9(b) and (d)). The Mg−10Gr and Mg−10MoS_2

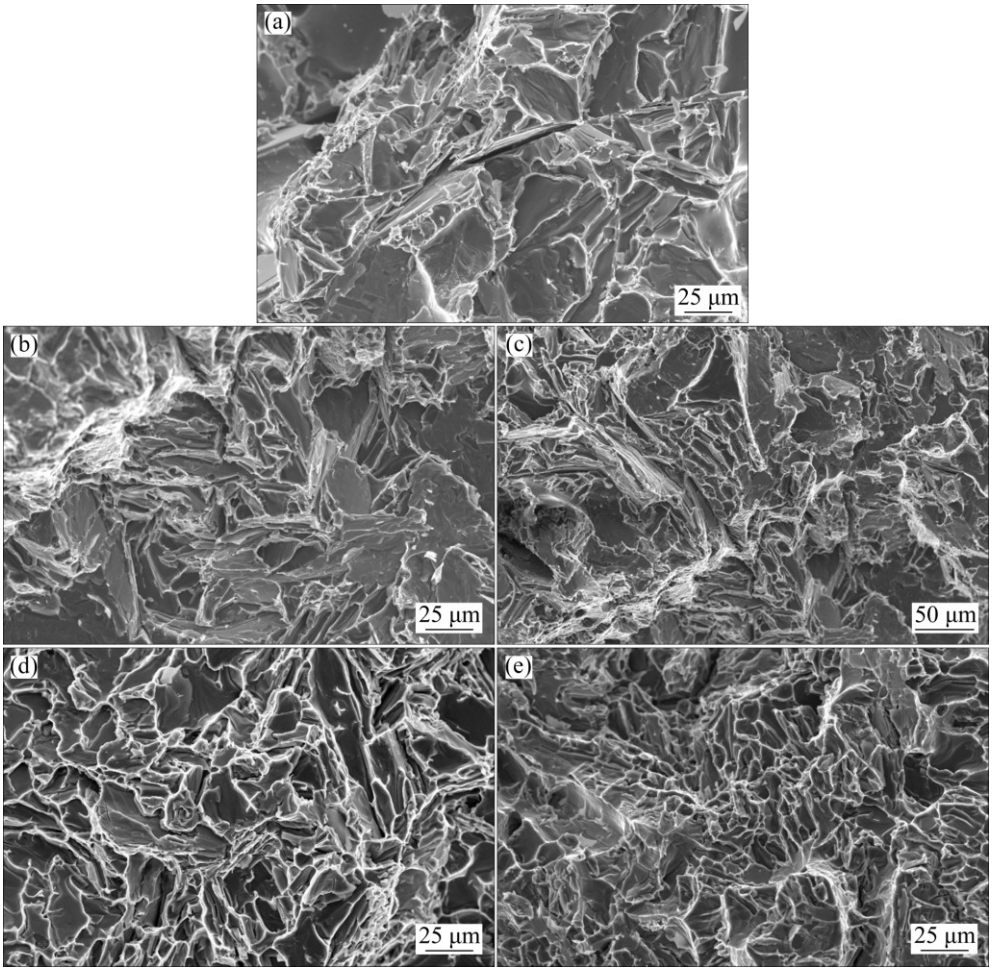

Fig. 7 Tensile fractographs of specimens Mg (a), Mg−5Gr (b), Mg−10Gr (c), Mg−5MoS_2 (d) and Mg−10MoS_2 (e)

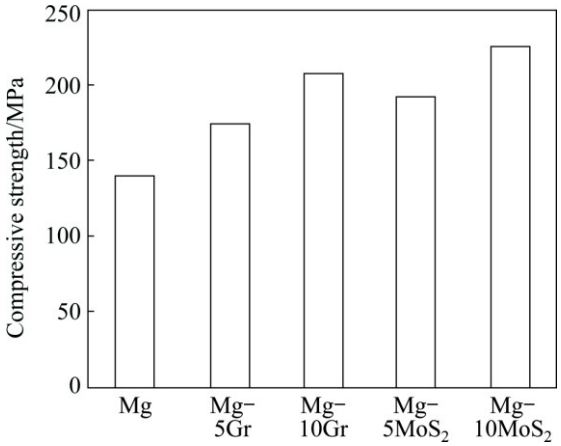

Fig. 8 Compression strength of prepared magnesium samples

composites show a combination of quasi-cleavage and more dimples, which implies a more malleable behaviour of the self-lubricating composites (Figs. 9(c) and (e)). The addition of solid lubricants above 5% causes a change on the fracture surface in the magnesium matrix, and increases the compressive strength of the self-lubricating composites. The fractured surfaces of the self-lubricating composites appear to be smoother than that of monolithic Mg (Fig. 9(a)) as seen in Figs. 9(b)−(e).

3.5 Effect of sliding load on friction and wear properties

To investigate the load effect on the tribological behaviour of the self-lubricating composites, they were tested at various loads of 2, 5, 10 and 15 N. Figure 10(a) shows the friction coefficient of Gr and MoS_2 of various compositions with sliding load at a constant distance of 2200 m and a sliding velocity of 3.14 m/s. The composite with solid lubricants prevented contact between the sliding surfaces, and the friction coefficient, therefore decreased with increasing contents of Gr and MoS_2 because the quantity of lubricant released between the mating surfaces increased, which reduced the friction coefficient. It was observed that as the mass fraction of the solid lubricant increased, the friction coefficient for both Mg−Gr and Mg−MoS_2 uniformly decreased.

This can be attributed to the fact that the existing lubricant film that formed on the worn surface

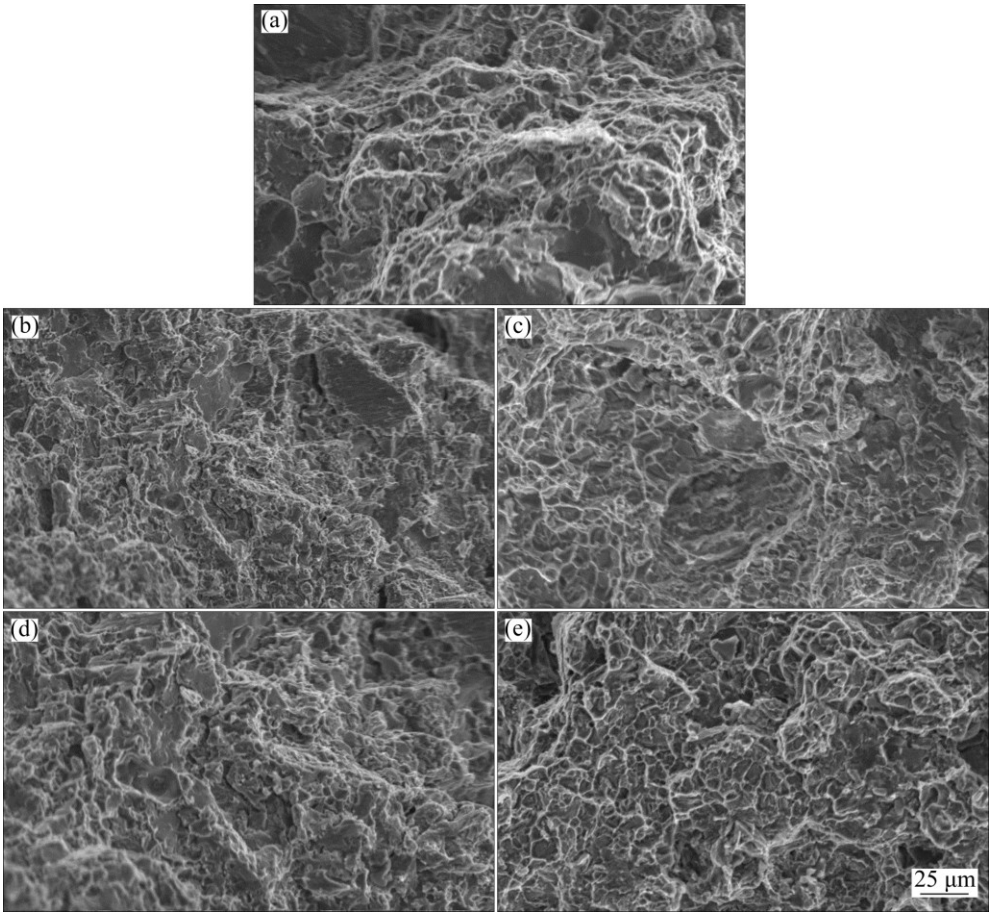

Fig. 9 Compressive fractographs of specimens Mg (a), Mg−5Gr (b), Mg−10Gr (c), Mg−5MoS_2 (d) and Mg−10MoS_2 (e)

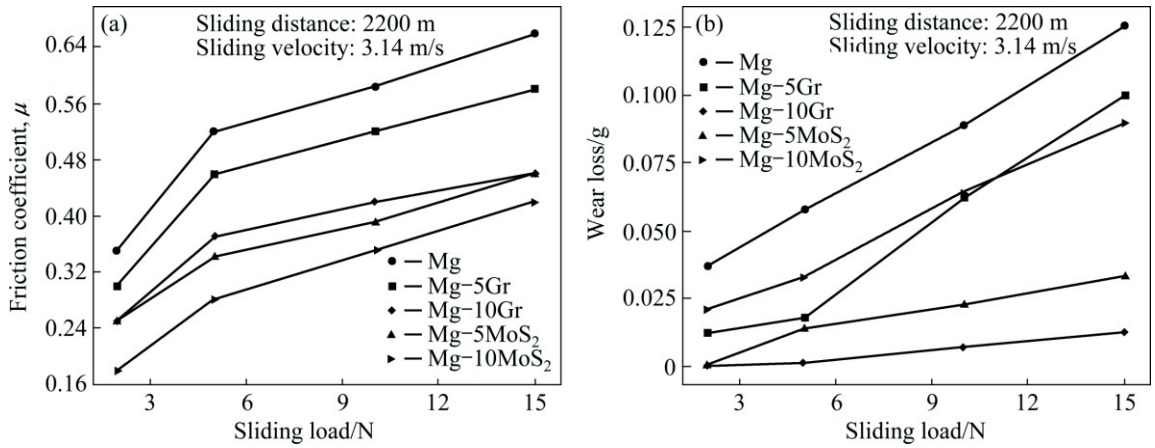

Fig. 10 Variations in friction coefficient (a) and wear loss (b) of prepared samples

progressively thickened as the mass fraction of Gr/MoS_2 increased. It can also be observed that the friction coefficient of all of the composites increased as the applied load increased, and the friction coefficient of the pure Mg was greater than that of the other composites at all applied loads. When comparing the composites, the Mg−10MoS_2 had the lowest friction coefficient. The variation in the wear loss of the composites with applied load is shown in Fig. 10(b). The wear loss of the composite specimens was significantly lower than that of the matrix shown in Fig. 10(b).

A lower wear loss occurred in the self-lubricating composites due to the presence of the second phase and increased density (Table 1), and the wear loss of the composites gradually decreased from 5% and 10% of the solid lubricants. The decreasing wear loss of the self-lubricating composites should be the result of the effect of the solid lubricants because Gr and MoS_2 are

too soft to support the counter face loads and permit rubbing between the pin and counter disk surfaces by forming a thin lubricating film. It is well known that the addition of 10MoS_2 increases the hardness, which contributes to the high wear resistance compared with that of the magnesium matrix. In addition, it was found that the wear loss of the unreinforced magnesium matrix and self-lubricating composites increased as the load increased.

3.6 Worn surface and wear debris analysis

Using the SEM, the wear tracks for the pure Mg matrix, Mg−Gr and Mg−MoS_2 composites were conducted. In Fig. 11(a), the worn surfaces are typified by large grooves along the sliding direction, due to wide-ranging wear caused by plastic deformation by abrasion, and hence severe wear is observed in the magnesium matrix. The wear was due to the sliding of the hard asperity counter disc surface over the softer magnesium matrix, which caused micro ploughing. No macroscopic transfer of layers on the counter face was observed on the worn surface.

The worn surfaces of Gr reinforced Mg composites after the dry sliding tests at 10 N are shown in Figs. 11(b) and (c). In the case of the Mg−5Gr composite, it can be observed that there are significant grooves and scars on the worn surface, which are shown in Fig. 11(b). In Fig. 11(c), it can be observed that the worn surface of the 10Gr reinforced composite was more consistently protected by the lubricating graphite film, which prevented the rubbing surfaces from coming into direct contact, and hence the film decreased the shear stress transferred to the sliding surface and decreased the friction coefficient and wear loss.

In the case of the Mg−MoS_2 composites, smaller grooves were observed on the worn surface along the sliding direction, as shown in Fig. 11(d). During sliding, the MoS_2 particles were smeared and formed a thin

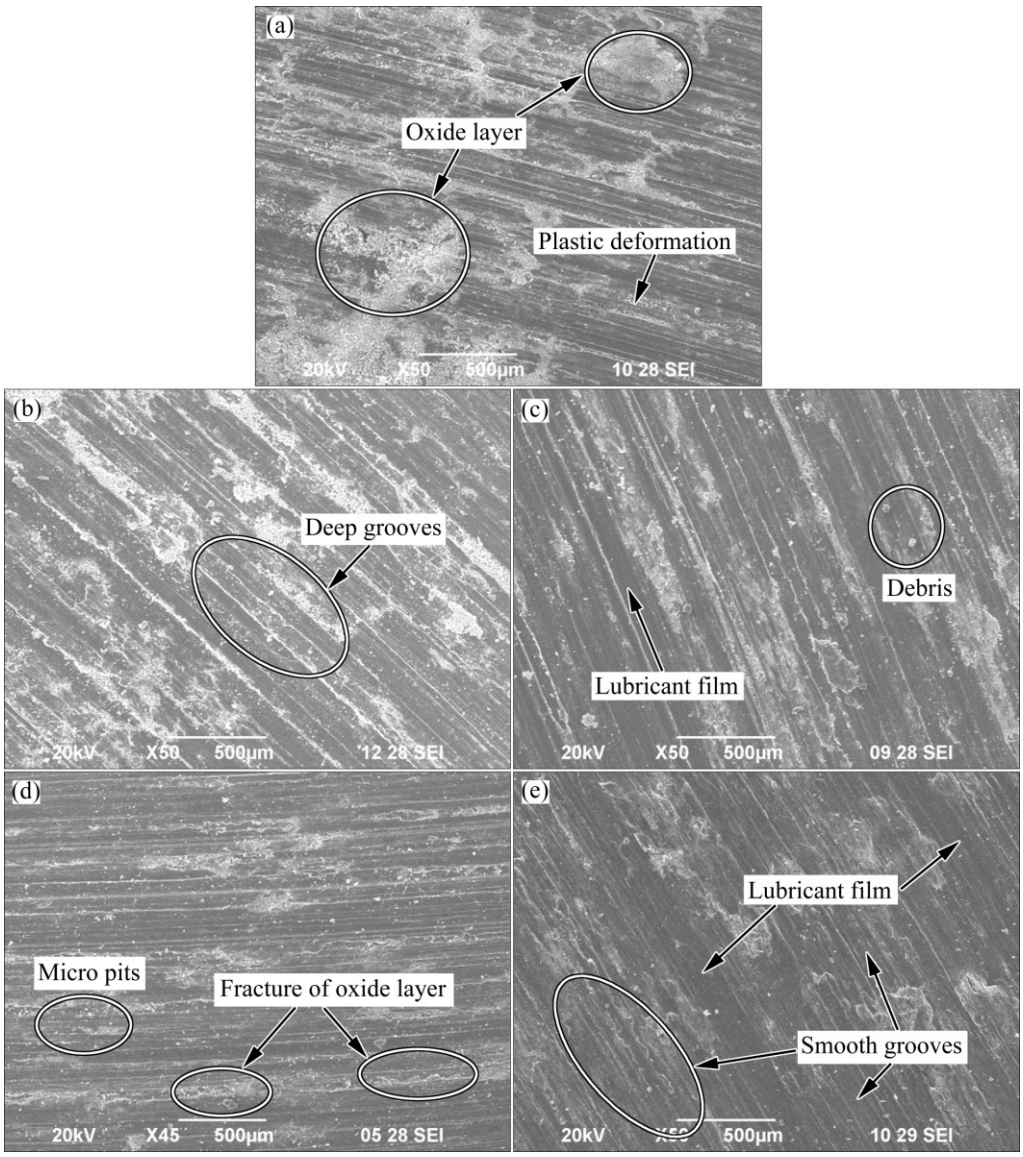

Fig. 11 SEM images of worn surfaces of Mg (a), Mg−5Gr (b), Mg−10Gr (c), Mg−5MoS_2 (d) and Mg−10MoS_2 (e)

lubrication film (Fig. 11(d)), which reduced the wear loss. Only small amounts of lubrication films were observed on the worn surface of the Mg−5MoS_2 composites. In Fig. 11(e), the composite with 10MoS_2 formed a larger amount of lubricant film on the worn surface.

The oxidation of MoS_2 during the wear process hastened the wear of the MoS_2 film lubricant. During sliding, the oxide layer was fractured, and MoS_2 particles were released from the worn surface. Even after a considerable degree of oxidation, MoS_2 was still able to deliver a satisfactory level of lubrication. The solid lubricants (Gr, MoS_2) were finally capable of decreasing the plastic deformation and abrasion of the worn surfaces. An oxidation wear mechanism was identified in the self-lubricating composites, and similar observations have been reported in previous studies [23,24].

The wear debris for the magnesium matrix was somewhat large (Fig. 12(a)), and the material was therefore softened, which led to easier removal of larger material removal and the formation of larger quantities and sizes of loose wear particle debris as a result of abrasive action. By the addition of Gr/MoS_2, the size of the wear debris was reduced and was smaller than that of pure magnesium (Figs. 12(b)−(e)). This decrease in the size of the wear debris was mainly caused by the high contents of Gr and MoS_2, which may have decreased the action of ploughing and delamination.

4 Conclusions

1) The self-lubricating magnesium composites has improved mechanical properties, preeminent wear resistances and friction coefficient compared with pure magnesium.

2) The hardness of the composites increased when reinforced with MoS_2, but the hardness decreased when reinforced with Gr, compared with the Mg matrix.

3) The metallography showed that the Gr and MoS_2

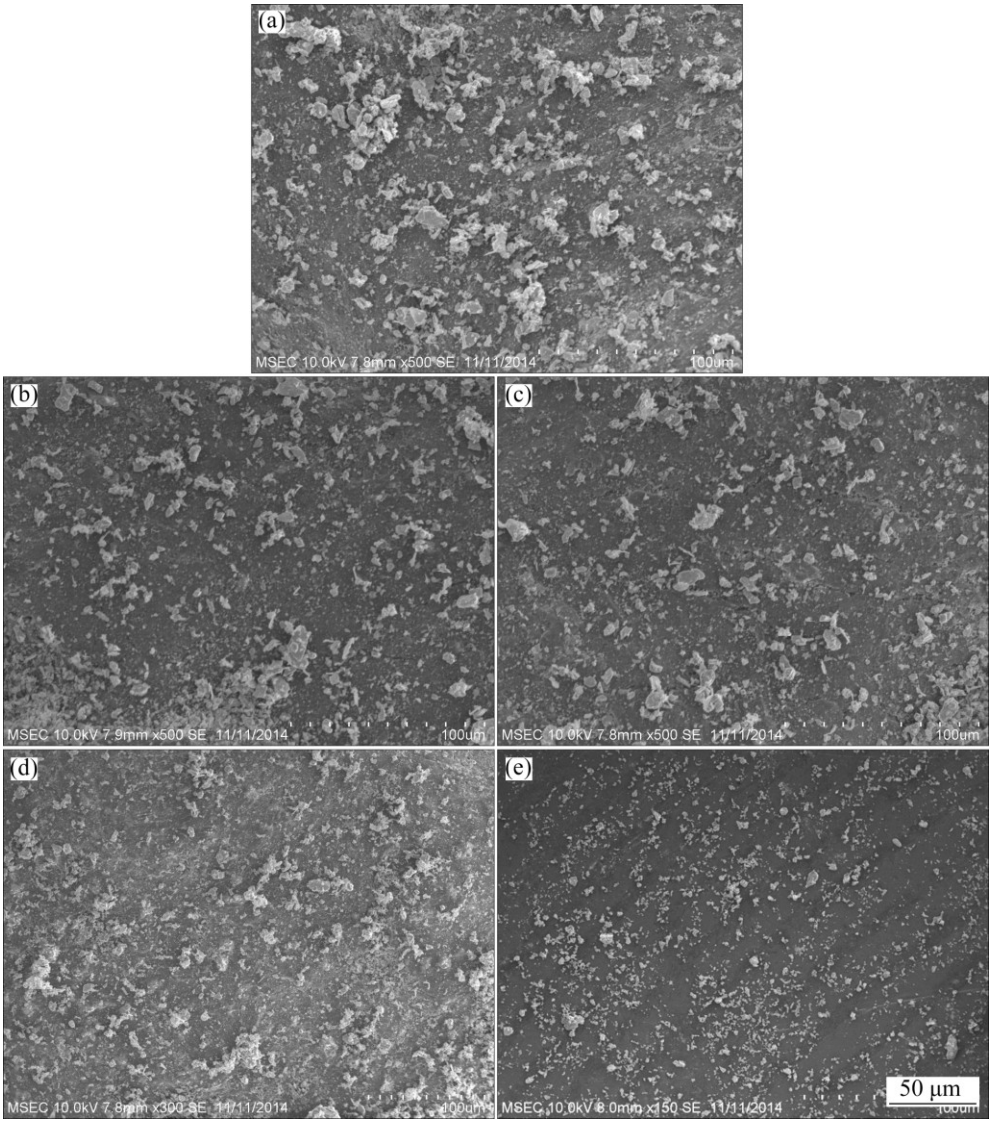

Fig. 12 SEM images of wear debris of Mg (a), Mg−5Gr (b), Mg−10Gr (c), Mg−5MoS_2 (d) and Mg−10MoS_2 (e)

particles were homogeneously dispersed within the magnesium matrix.

4) The addition of MoS_2 solid lubricants at all mass fraction improved the hardness, tensile and compressive strength and tribological properties over that of Gr.

5) For both of the solid lubricants, the friction coefficient depended on sliding load, and the friction coefficient increased with increasing sliding loads.

6) MoS_2 rather than Gr reduced the friction coefficient and wear more effectively. The best combination of hardness, compressive strength and tensile strength was achieved using Mg−10MoS_2 composite.

7) The self-lubricating magnesium composites have significant potential in diverse engineering applications, such as defence and military operations.

References

[1] KULEKCI M K. Magnesium and its alloys applications in automotive industry [J]. The International Journal of Advanced Manufacturing Technology, 2008, 39: 851−865.

[2] MORDIKE B L, EBERT T. Magnesium: Properties-applications-potential [J]. Materials Science and Engineering A, 2001, 302: 37−45.

[3] LANDKOF B, KAINER K U. Magnesium alloys and their applications' [M]. Weinheim: Wiley–VCH Verlag, 2000: 168.

[4] MORDIKE B L, EBERT T. Magnesium: Properties – applications – potential [J]. Material Science and Engineering A, 2001, 302: 37−45.

[5] HU Yong, RAO Li. Effect of particulate reinforcement on wear behavior of magnesium matrix composites [J]. Transactions of Nonferrous Metals Society of China, 2012, 22: 2659−2664.

[6] YAO Yan-tao, JIANG Lan, FU Gao-feng, CHEN Li-qing. Wear behavior and mechanism of B4C reinforced Mg-matrix composites fabricated by metal-assisted pressureless infiltration technique [J]. Transactions of Nonferrous Metals Society of China, 2015, 25: 2543−2548.

[7] GUPTA M, SHARON N M L. Magnesium, magnesium alloys and magnesium composites [M]. Hoboken: John Wiley & Sons Inc, 2011.

[8] PRAMANIK A. Effects of reinforcement on wear resistance of aluminum matrix composites [J]. Transactions of Nonferrous Metals Society of China, 2016, 26: 348−358.

[9] RAM PRABHU T. Effects of solid lubricants, load, and sliding speed on the tribological behaviour of silica reinforced composites using design of experiments [J]. Materials and Design, 2015, 77: 149−160.

[10] CAI Bin, TAN Ye-fa, TU Yi-qiang, WANG Xiao-long, TAN Hua. Tribological properties of Ni-base alloy composite coating modified by both graphite and TiC particles [J]. Transactions of Nonferrous Metals Society of China, 2011, 21: 2426−2432.

[11] LI Jing-fu, ZHANG Lei, XIAO Jin-kun, ZHOU Ke-chao. Sliding wear behavior of copper-based composites reinforced with graphene nanosheets and graphite [J]. Transactions of Nonferrous Metals Society of China, 2015, 25: 3354−3362.

[12] MIYAJIMA T, TANAKA Y, IWAI Y, KAGOHARA Y, HANEDA S, TAKAYANAGI S, KATSUKI H. Friction and wear properties of lead-free aluminium alloy bearing material with molybdenum disulfide layer by a reciprocating test [J]. Tribology International, 2013, 59: 17−22.

[13] ZHANG Xiao-feng, ZHANG Xiang-lin, WANG Ai-hua, HUANG Zao-wen. Microstructure and properties of HVOF sprayed Ni-based submicron WS_2/CaF_2 self-lubricating composite coating [J]. Transactions of Nonferrous Metals Society of China, 2009, 19: 85−92.

[14] RAVINDRAN P, MANISEKAR K, NARAYANASAMY P, SELVAKUMAR N, NARAYANASAMY R. Application of factorial techniques to study the wear behaviour of Al hybrid composites with graphite addition [J]. Materials and Design, 2012, 39: 42−54.

[15] BRUDNYI A I, KARMADONOV A F. Structure of molybdenum disulphide lubricant film [J]. Wear, 1975, 33: 243−249.

[16] WANG Juan, FENG Yi, LI Shu, LIN Shen. Influence of graphite content on sliding wear characteristics of CNTs−Ag−G electrical contact materials [J]. Transactions of Nonferrous Metals Society of China, 2009, 19: 113−118.

[17] XUE Qun-ji, BAI Ming-wu. Tribological properties of SiC whisker and molybdenum particle-reinforced aluminium matrix composites under lubrication [J]. Wear, 1996, 195: 66−73.

[18] KOVACIK J, EMMER S, BIELEK J, KELESI L. Effect of composition on friction coefficient of Cu-graphite composites [J]. Wear, 2008, 265: 417−421.

[19] HIROTAKA K, MASAHIRO T, YOSHIRO I, KAZUO W, YOSHINORI S. Wear and mechanical properties of sintered copper–tin composites containing graphite or molybdenum disulfide [J]. Wear, 2003, 255: 573−578.

[20] RAVINDRAN P, MANISEKAR K, NARAYANASAMY R, NARAYANASAMY P. Tribological behavior of powder metallurgy-processed aluminium hybrid composites with the addition of graphite solid lubricant [J]. Ceramics International, 2013, 39: 1169−1182.

[21] RAVINDRAN P, MANISEKAR K, RATHIKA P, NARAYANASAMY P. Tribological properties of powder metallurgy– processed aluminium self-lubricating hybrid composites with SiC additions [J]. Materials and Design, 2013, 45: 561−570.

[22] ZHANG Mei-juan, YANG Xiao-hong, LIU Yong-bing, CAO Zhan-yi, CHENG Li-ren, PEI Ya-li. Effect of graphite content on wear property of graphite/Al_2O_3/Mg−9Al−1Zn−0.8Ce composites [J]. Transactions of Nonferrous Metals Society of China, 2010, 20: 207−211.

[23] NARAYANASAMY P, SELVAKUMAR N, BALASUNDAR P. Effect of hybridizing MoS_2 on the tribological behaviour of Mg−TiC Composites [J]. Transactions of the Indian Institute of Metals, 2015, 68: 911−925.

[24] SELVAKUMAR N, NARAYANASAMY P. Optimization and effect of weight fraction of MoS_2 on the tribological behaviour of Mg−TiC−MoS_2 hybrid composites [J]. Tribology Transactions, 2016, 59: 733−747.

自润滑烧结镁基复合材料的拉伸、压缩和磨损行为

P. NARAYANASAMY[1], N. SELVAKUMAR[2]

1. Department of Mechanical Engineering, Kamaraj College of Engineering and Technology, Virudhunagar 626001, Tamilnadu, India;
2. Department of Mechanical Engineering, Mepco Schlenk Engineering College, Sivakasi 626005, Tamilnadu, India

摘　要：采用粉末冶金方法制备石墨/二硫化钼增强镁基自润滑复合材料，并分别表征这些复合材料的显微组织、物理性能、力学性能和磨损性能。利用 XRD 手段鉴定复合材料中的 Gr/MoS_2 相。显微组织观察表明，Gr/MoS_2 颗粒均匀地分散在镁基体中。在室温条件下施加载荷 5 g 并保持 15 s，测试复合材料的显微硬度，得到所有复合材料的显微硬度为 VHN 29−34。使用显微硬度、拉伸和压缩试验研究材料的力学性能，并用扫描电子显微镜分析材料的断口形貌，得到 Mg−10MoS_2 复合材料最高的硬度、抗压强度和拉伸强度。用销−盘式摩擦仪测试烧结复合材料的摩擦因数和磨损量。另外，通过磨损表面特征，利用 SEM 系统分析复合材料的摩擦磨损机制。结果表明，与石墨相比，二硫化钼的摩擦因数和磨损有所减少。

关键词：镁合金复合材料；自润滑；粉末冶金；滑动磨损；显微组织；力学性能

(Edited by Xiang-qun LI)